https://doi.org/10.5194/wes-2024-68
Preprint. Discussion started: 28 June 2024

eawe european academy of wind energy
Open Access WIND ENERGY SCIENCE DISCUSSIONS

Probabilistic lifetime extension assessment using mid-term data: Lillgrund wind farm case study

Shadan Mozafari[1,*], Jennifer Marie Rinker[1], Paul Veers[2], and Katherine Dykes[1]

[1]Department of Wind Energy, Technical University of Denmark, Roskilde, Denmark
[2]National Renewable Energy Laboratory (NREL), Golden, CO, USA.

Correspondence: Shadan Mozafari (Shad.mzf@gmail.com)

Abstract.

Estimating the site-specific fatigue reliability of wind turbines is an integral part of probabilistic lifetime extension assessment. Limitations in type, accuracy, and availability of site-specific data is one of the main challenges in such estimations. The present research tackles the challenge of estimating long-term fatigue loads using short-term strain gauge measurements via statistical extrapolation. The case study wind turbine is a Siemens 2.3MW, in the Lillgrund wind farm, located in the Øresund strait between Denmark and Sweden. The turbine is heavily instrumented and Supervisory Control and Data Acquisition (SCADA) is also available. The study also reassesses the performance of the Frandsen model—as a simplified approach for estimating higher turbulence due to wakes — in a compact wind farm layout using aeroelastic simulations of the case study wind turbine. Furthermore, it shows the sensitivity of the site-specific reliability with respect to the uncertainty in material strength, fatigue load, and damage accumulation model.

The results reveal that for the case-study site, the Frandsen model underestimates turbulence in below-rated mean wind speeds and overestimates the turbulence in above-rated mean wind speeds. However, using the Frandsen model for estimating the long-term fatigue loads in the case study location leads to a 35% lower reliability index than a site-specific assessment using data from the SCADA system and, thus, is relatively more conservative. The study reveals that the sensitivity of the fatigue reliability to the load's uncertainty is negligible in assessment using site measurements and relatively high when using the Frandsen model.

The extrapolation approach used in the current study can facilitate the use of digital twins when strain gauge measurements are unavailable for a part or the whole span of the lifetime. In addition, the assessment of the Frandsen model in the case study wind farm, as an example of a wind farm with short spacing, adds valuable information to the ongoing studies in the literature about the performance of the model in intense and mixed-waked conditions. Finally, the provided information about robustness of the reliability based on the load estimation approach, is useful for considering uncertainty in the lifetime extension assessment.

keywords: Frandsen model, Lifetime extension, Wind farm, Fatigue reliability, Wind turbine wakes, Statistical extrapolation

https://doi.org/10.5194/wes-2024-68
Preprint. Discussion started: 28 June 2024

eawe european academy of wind energy
Open Access WIND ENERGY SCIENCE DISCUSSIONS

1 Introduction

Exposure of the wind turbines within a wind farm to the wakes increases their fatigue loads (Kim et al. , 2015; Lee et al. , 2013; Frandsen , 2007). The tower and foundations are often designed based on site-specific conditions, while in the case of the rotor-nacelle assembly, only the site suitability is checked to ensure safety during the design life. The IEC standard's design requirements often involve conservative assumptions. In fact, the requirements are often conservative enough to seek an extension of the operation time even after experiencing the high fatigue loads caused by wakes in the wind farm. Extending the operation time above the design service life (typically 20-25 years), in cases where maintaining safety is possible, is environmentally beneficial and can reduce the levelized cost of energy (Dimitrov and Natarajan , 2020; Natarajan et al. , 2020). IEC 61400-1 (2019) suggests the Frandsen model (Frandsen , 2007; Frandsen and Madsen , 2003) for site suitability checks. The Frandsen model involves simplified assumptions, and, thus, has some limitations. Bayo and Parro (2015) mention the following as some examples of the limitations:

- The model provides no prescription for the wake interaction from different wind turbines.
- The turbulence intensity in the model is normalized to the free stream wind speed rather than the local wind speed at the position of interest (Argyle et al., 2018). Thus, the model can be under-conservative when the farm highly impacts the mean wind speed.

Therefore, in wind farms with compact/irregular arrangements, ensuring the performance of the Frandsen model for conservative site-suitability checks is crucial.

Despite all the studies on the performance check of the Frandsen model, the performance in the high-mixed wake conditions due to small spacing and irregular layouts has not been studied. Lillgrund wind farm has a very compact layout (small spacing between the wind turbines), causing strong wake effects. Thus, it is a perfect case study for investigating the Frandsen model's validity in such conditions.

Another challenge for assessing site-specific assessment of the lifetime is data limitation. When assessing the possibility of lifetime extension, one often has to estimate the damage in time spans longer than the duration of the measurements. How to determine the turbine-specific fatigue damage accumulated throughout the operation time based on above-mentioned limitations is still an important question. The importance is especially high for the offshore wind industry due to the high scatter of environmental data in offshore conditions.

Some studies, including (Amiri et al., 2019) and (Ziegler and Muskulus , 2016), perform the lifetime extension assessment by assuming a linear damage increase through time. Such an approach can introduce errors in the estimations when the available data are insufficient to estimate the damage equivalent load (DEL) accurately. Although DEL is an averaged variable and thus is more robust to individual occurrences (Mozafari et al. , 2023b), it can still vary in different lengths of data for

https://doi.org/10.5194/wes-2024-68
Preprint. Discussion started: 28 June 2024

the components with high fatigue exponents. The results of (Mozafari et al. , 2023a) illustrate that the conventional approach of assuming the constant DEL, i.e., linear damage increase through time, can introduce bias in the long-term fatigue damage assessment in the case of the blade due to the composite's high fatigue exponent.

To generate long-term fatigue loads using mid-term measurements, some researches like (Dimitrov and Natarajan , 2019; Natarajan et al. , 2020) have used machine learning techniques and methods like Monte-Carlo simulations. Some studies like Ling et al. (2011); Hübler et al. (2018); Natarajan (2022) use stochastic methods to anticipate long-term data based on mid-term measurements. Having such methods facilitate using digital twins of the wind turbines within the wind farm for assessment of the lifetime extension using SCADA data. Despite different statistical approaches and the guidelines give in (IEC 61400-1 , 2019), there is not enough clarity on how to statistically extrapolate the fatigue loads. The current work reproduces a database accounting for long-term DEL up to 30 years return period loads by fitting the Gamma mixture model to the mid-term measurements.

We assesses the possibility of a ten-year lifetime extension for one of the wind turbines at the edge of the Lillgrund wind farm while maintaining acceptable safety margins. The case-study wind turbine is exposed to both non-waked and different scenarios of waked streams. First, using the available SCADA data, we study the performance of the Frandsen model in the safe estimation of the loads in the case study wind farm. We bin the different wake scenarios around the case study wind turbine for a more detailed assessment of Frandsen model turbulence estimations. The study uses the Gamma mixture model to assess the remaining useful life using 10-minute strain gauges DEL measurements in the blade root by reproducing a database accounting for long-term DEL up to 30 years return period loads. In addition, it performs a sensitivity study to investigate the relative importance of the loads, material fatigue strength, and damage accumulation rule in fatigue reliability estimation in different scenarios: site, Frandsen model, and the IEC design requirements. Awareness about the share of different sources of uncertainty on the assessment of lifetime extension in case of using the Frandsen model or site measurements is valuable. One must consider that the material properties are calibrated such that the target reliability level of 3.7 ISO-2394 (2015) is reached after 20 years based on design class. Thus, although the comparisons of the reliability levels are correct, the levels are not.

In the next sections, first, we present the methods and models we use for modeling and reliability assessment in Sect. 2. Then we present the results and corresponding discussions of the Frandsen performance check and lifetime extension assessments in Sect. 3. Finally, in Sect. 4, we present the conclusions of both studies and suggestions for future studies.

2 Methodology

First, we introduce the case study wind turbine and the corresponding wind farm in Sect. 2.1 and Sect. 2.2, respectively. Then, in section 2.3, we present the setup and features of the aeroelastic simulations and site measurements. In addition, we introduce

https://doi.org/10.5194/wes-2024-68
Preprint. Discussion started: 28 June 2024

eawe european academy of wind energy
Open Access WIND ENERGY SCIENCE DISCUSSIONS

the methods we use for assessing and filtering data for the current study. Finally, in section 2.4, we introduce the mathematical formulas and the procedures we use for post-processing the simulation results and measurements.

2.1 The case study wind turbine

The wind turbine under study in the current research is SWT-2.3-93, manufactured by what is now Siemens Gamesa Renewable Energy (SGRE). The turbine has a 92.6-meter rotor diameter, a hub height of 65m, and a rated power of 2.3 MW. The cut-in and cut-out mean wind speeds are 3 m/s and 25 m/s, respectively, reaching the nominal power at approximately 12-13 m/s. The turbine belongs to class 1A based on the IEC 61400-1 standard's classification.

2.2 The case study wind farm

The strain-gauge and environmental measurements belong to one of the turbines in the edge of the Lillgrund offshore wind farm. Lillgrund wind farm is located about 10 km off the coast of Sweden in the Öresund region and consists of 48 Siemens SWT-2.3 93 wind turbines (total capacity of 110 MW). The turbines are placed in an 8×8 arrangement with two empty spots in the middle of the layout as shown in Fig. 1. The circles in Fig. 1 represent different turbines, and the red circle is the case study wind turbine, denoted as C08 (row c and column 8). We bin the wind directions around the case study wind turbine to roughly distinguish between different wake conditions. The binning facilitates assessing the performance of the Frandsen model and IEC NTM assumptions in characterizing turbulence in different wake scenarios. The dashed lines in Fig. 1 show the bins. For the rest of the study, we refer to the wind direction bins as 'wind bins' for simplicity.

As Fig. 1 illustrates, wind bin 1 accounts for non-waked conditions. In wind bins 2, 3, and 7, the stream is mainly passing by a single turbine, with bin 3 representing a relatively long distance between the turbine generating the wake and the C08 wind turbine. Wind bin 5 is an intense condition, with the case study turbine being very deep in the row and a very short distance between the closest wind turbine (4.3D). Bin 4 is a similar arrangement of a single row with a relatively long distance, and bin 6 is a mixed-waked flow condition. One should note that the binning and the corresponding conditions described are rough and are only used for general comparison.

2.3 Measurement data and aeroelastic simulations

In the present study, we use SCADA and 10-minute DEL evaluations extracted from a strain gauge installed on the blade root. The data represent long duration measurements in a span of 5 years in the Lillgrund wind farm. We also perform three groups of aeroelastic simulations in HAWC2 software (Larsen and Hansen , 2007): Group 1 based on IEC 61400-1 design requirements for wind turbine class A, Group 2 based on Frandsen's effective turbulence model (model explained in 2.4), and Group 3 based on site SCADA measurements in the non-waked wind directions for validation of the wind turbine model. In the following, first, we introduce the available measurement data (from the strain gauge and SCADA). Then, we present the specifications of the three groups of aeroelastic simulations.

https://doi.org/10.5194/wes-2024-68
Preprint. Discussion started: 28 June 2024

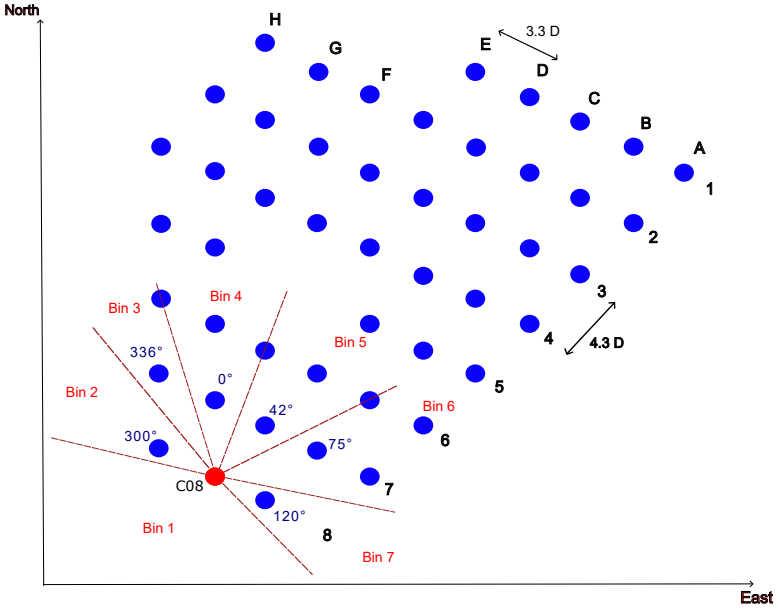

Figure 1. Arrangement of the wind turbines in the Lillgrund wind farm and the wind direction bins around the turbine C08 used in the current study

2.3.1 Measurement data

The available data are an integration of strain gauge data and SCADA data, including sensor measurements of wind speed, wind direction, power production, and rotor speed. The mean and standard deviation of wind are derived based on an anemometer installed on met mast very close to the case study wind turbine. In addition, the strain gauge is installed at 1.5 m away from the blade root. All data are measured in time intervals of ten minutes during years 2008 to 2012. The strain gauge measurements are transformed into 10-minute DELs using the Palmgren-Miner approach, considering Wöhler exponent equal to ten for the composite structure of the blade. The measurement campaign only covers around two years and not the full 5-year period (see Fig. B1 for the scatter of data during five years). Although the non-operational conditions should also be considered for fatigue assessments, in the current study, we only focus on normal operating conditions in the simulations (DLC 1.2 in the IEC standard). We use the provided DEL data to estimate the site-specific fatigue loads for the comparison study after filtration. We filter the data not only to derive reliable wind measurements but also to filter out non-operational conditions (as they are not within the scope of the current study). We use the power curve of the turbine and utilize the data from SCADA, including mean wind speed, mean rotor speed, and the mean power production for the same points of time to exclude the DEL data that do not represent the operational conditions (Fig. C1 in the appendix shows the power curve after such filtration).

https://doi.org/10.5194/wes-2024-68
Preprint. Discussion started: 28 June 2024

eawe european academy of wind energy
Open Access WIND ENERGY SCIENCE DISCUSSIONS

Table 1 shows the normalized number of data available in different wind direction bins around the C08 wind turbine (see the bins in 1) after filtration. In addition, table 1 shows the probability of occurrence of each bin based on the wind rose of the site (Vitulli et al. , 2019).

Table 1. Binning of wind directions and their corresponding probability in the Lillgrund wind farm site based on Vitulli et al. (2019)

Bin number	Wind direction bounds (degrees)	Probability (%)	Normalized number of available data
1	135-285 (non-waked)	55.5	0.5656
2	285-315	9.6	0.0741
3	315-345	5.0	0.0715
4	345-360, 0-15	5.4	0.0298
5	15-60	6.9	0.0623
6	60-105	9.3	0.1261
7	105-135	8.3	0.0851

As Table 1 illustrates, the available data after filtration do not fully cover the wind direction probabilities. This is partly because in some heavily waked conditions, the turbine has been shut down and partly because of the short duration of the data gathering. In the current work, we keep the mentioned observation in mind as a limitation. Thus, we proceed with assessing all DEL data together in fitting, extrapolation, and bootstrapping the samples. Fig. D2 (in appendix) shows the separate analysis of the DEL data in each wind direction bin. The analysis shows the rank of each wind bin in terms of the highest DEL observation and expectations. This analysis should be considered when accounting for fatigue assessments in each bin for more accurate assessments. However, as mentioned, in the current study, we estimate the damage accumulations based on assessment of the gross data. This limitation is discussed further in Sect. 4. The wind standard deviation (turbulence) data are used directly for fitting of the corresponding probability distributions in the turbine's location. We sample from the distributions and use them as input for aeroelastic simulations in the second part of the study (see Sect. 2.3.2).

2.3.2 Aeroelastic simulations

The current work includes three main simulation groups. Group 1 is based on inputs from IEC 61400-1 requirements for design. Group 2 is based on the IEC 61400-1 recommendation for site suitability check, i.e., the Frandsen model. Group 3 is based on the site-specific inputs in terms of turbulence and wind shear exponent from the free stream (wind bin 1 in Fig. 1). The third group of simulations is only used for validation of the HAWC2 turbine model. The results of the validation checks are provided in the appendix.

Groups 1 and 2 have 11 mean wind speed bins (from 4m/s up to 24m/s with 2m/s intervals). Group 3 only includes the mean wind speeds up to 20 m/s as the number of data points and probability of occurrence for the higher mean wind speeds are very low. The two first groups of simulations have one representative turbulence level in each mean wind speed bin. This level equals the 90% quantile value in group 1 and the Frandsen waked turbulence level in group 2 (more details are provided in the

https://doi.org/10.5194/wes-2024-68
Preprint. Discussion started: 28 June 2024

eawe european academy of wind energy
Open Access WIND ENERGY SCIENCE DISCUSSIONS

next section).

We consider 100 seeds for each wind condition to account for the variability of the wind (Mozafari et al. , 2023b) and have enough data for fitting distributions to the resulted DELs. The third group includes 20 samples from the site-specific turbulence standard deviation distribution in each mean wind speed in the free stream (wind bin 1). In this group, having nine mean wind speeds in the related wind directions, and 100 turbulence seeds for each turbulence level resulted in a total number of 22000 simulations of 10min duration for the site-specific aeroelastic simulations (group 3). Considering a lognormal wind profile in all simulations, we consider the exponent equal to 0.2 in the first two groups and equal to 0.1 in group 3. We use the Mann turbulence model (Mann , 1998) to generate the simulation turbulence boxes. The boxes contain 8192 evaluation points alongside the wind direction for higher resolution and 32 points in the other two directions. Table 2 shows the specifications of each group of aeroelastic simulations.

Table 2. Specifications of wind modeling in three groups of Hawc2 simulations corresponding to three study cases

Parameter	**Group 1**	**Group 2**	**Group 3**
Turbulence in each mean wind speed	90% quantile in NTM	Frandsen's effective turbulence	Ambient turbulence distribution
Reference turbulence intensity	0.16	-	0.11
Turbulence levels in each MWS bin	1		20
Wind shear coefficient	0.2		0.1
Realizations per wind condition	100		
Turbulence model	Mann		
Cut-in mean wind speed (m/s)	4		
Cut-out mean wind speed (m/s)	26		
Rated wind speed (m/s)	11.4		
size of wind speed bins (m/s)	2		
Yaw angle (degrees)	0		
Mann box grids along the wind	8192		
Mann box grids in other dimensions	32		
Simulation length (sec.)	700		
Transient time (sec.)	100		
Time steps of the simulations (sec.)	0.01		

The following section includes the mathematical relations and procedures used in the study.

https://doi.org/10.5194/wes-2024-68
Preprint. Discussion started: 28 June 2024

eawe european academy of wind energy
Open Access WIND ENERGY SCIENCE DISCUSSIONS

2.4 Mathematical formulations

In the current section, first, we introduce the wind characteristics, and then we briefly present the relations for fatigue load assessment plus methods for the reliability and sensitivity analysis. Finally, we explain the procedure for forming the database for statistical extrapolation of DEL measurements via bootstrapping.

2.4.1 Probabilistic modelling of wind

In the current study, we only observe two random parameters of the wind field: mean wind speed and the wind speeds' standard deviation (turbulence). We consider the rest of the parameters as constants in the simulations. Following the IEC standard (IEC 61400-1 , 2019), we assume the distribution of the mean wind speed at hub height to be Reighley for both cases of design-level assessment and site-suitability check (the Frandsen model). In both these cases, the mean wind speed in the waked area is assumed to be the same as the free stream. In the case of site-specific assessment in non-waked conditions, we assume the same distribution as it complies with reality on the site. In the case of design-based assessment, we use 90% quantile of the lognormal distribution as suggested by the Normal Turbulence Model in IEC 61400-1 (2005) as the representative turbulence. Equation 1 presents this level.

$$\sigma_{rep.design} = I_{ref}(0.75 v_{hub} + 5.6) \tag{1}$$

In Eq. 1, I_{ref} is the reference turbulence intensity equal to 0.16 for the standard class 1 wind turbines (the current case study). In addition, V_{hub} is the hub height wind speed.

In the Frandsen model, the free stream standard deviation is assumed to be the 90% quantile of a normal distribution (Argyle et al., 2018). In the waked conditions, the turbulence is described as a function of the thrust coefficient and the normalized distance of the closest wind turbine. Equation 2 and Eq. 3 present the free stream standard deviation formulations and enhanced turbulence due to wakes in the Frandsen model.

$$\sigma_{rep.Frandsen} = \mu_\sigma + 1.28 * \sigma_\sigma \tag{2}$$

In Eq. (2), σ is the turbulence standard deviation of the free stream (ambient flow) and μ_σ and σ_σ refer to the mean and standard deviation of this parameter, respectively.

$$T_{waked}(\theta) = \sqrt{\frac{v_{hub}^2}{\left(1.5 + 0.8\left(\frac{di(\theta)}{\sqrt{C_T}}\right)\right)^2} + \sigma_{rep.Frandsen}^2} \tag{3}$$

The Frandsen model's turbulence is the same in all wind directions (like in IEC design assessments). This independence from wind direction is obtained by effective turbulence. Equation 4 shows the effective turbulence used for site-suitability check (IEC 61400-1 , 2019).

https://doi.org/10.5194/wes-2024-68
Preprint. Discussion started: 28 June 2024

eawe european academy of wind energy
Open Access WIND ENERGY SCIENCE DISCUSSIONS

$$T_{eff}(V_{hub}) = \left(\sum_{\theta=0}^{2\pi} P_{\theta}(V_{hub}) T_{waked}(\theta) \right)^{\frac{1}{m}} \tag{4}$$

We use the thrust coefficient data provided in (Montavon et al. , 2009) for the current study.

2.4.2 DEL estimation

In the present research, we use the Basquin relation (Basquin , 1910) for modeling the fatigue resistance of the composite material and Palmgren–Miner (Miner's) rule (Palmgren , 1924; Miner , 1945) for modeling the damage accumulation. These models describe the lifetime and damage as functions of stress, while the outputs of the aeroelastic simulations that we use are flapwise bending moments in the blade root. Since the location of the interest (the strain-gauge installation location) is close to the root and nearly circular, we use Eq. 5 to obtain the stresses based on the moment time series.

$$S_i = \frac{Mx_i c}{Iy} \tag{5}$$

In Equation 5, Mx_i is the moment corresponding to the stress level S_i. In the current study, the direction y corresponds to the global direction of the wind in the HAWC2 simulations. Thus, we consider moments in the perpendicular direction (Mx). In addition, the section parameters c and I_y are the radius (half of the chord) and the moment of inertia in the direction perpendicular to the moment's direction, respectively. The corresponding values are not mentioned here because of confidentiality.

Using rain flow counting (Endo et al. , 1967) of the moments in each 10-minute simulation and the models mentioned (Basquin and Palmgren–Miner), we estimate the 10-minute fatigue damage via Eq. 6.

$$D = \left(\frac{c}{I_y} \right)^m \sum_{i=1}^{Ns} \frac{n_i Mx_i^m}{k} \tag{6}$$

Reformulation of the Eq. 6 using the concept of damage equivalent load (DEL) (see Mozafari et al. (2023b) for more information) results in Eq. 7. We use this expression in the current study to simplify the comparisons.

$$D = \frac{Neq(DEL_{lifetime}^m)}{k} \left(\frac{c}{I} \right)^m \tag{7}$$

In Eq. (7), N_{eq} is the reference number of cycles. we set N_{eq} equal to 600 cycles corresponding to the average of 1Hz. Cyclic loading. In addition, $DEL_{lifetime}$ (The expected value of the fatigue damage equivalent load through lifetime)can be derived from 10-minute DEL estimations via Eq. 8.

$$E[DEL_{lifetime}^m] = \sum_{\Theta=\Theta_L}^{\Theta_U} \sum_{V_\Theta=V_L}^{V_U} \sum_{T_{(\Theta,V)}=T_L}^{T_U} E[(DEL_{10-min,\Theta})^m] \mathrm{P}(T,V|\Theta) \mathrm{P}(\Theta) \tag{8}$$

https://doi.org/10.5194/wes-2024-68
Preprint. Discussion started: 28 June 2024

In Eq. (8), the parameters Θ_L and Θ_U, V_L, and V_U, as well as t_L and t_U, represent the lower bound and higher bound for mean wind speed and turbulence in each wind bin. Furthermore, $\mathrm{P}(T,V|\Theta)$ is the joint probability of turbulence and mean wind speed bins conditioned on different direction bins. Since we are considering the marginal probability of turbulence conditioned on the mean wind speed bin, and the probability of each mean wind speed conditioned on the direction, the joint probability equals the multiplication of the three marginal probabilities. In the case of assessments with constant turbulence in each mean wind speed (Frandsen effective and IEC representative turbulence characterization), the probability of the single turbulence level equals 1. In the case of group 3 simulations, we account for the probability distribution of turbulence in each wind speed bin, and the probability of the wind direction bin is set to 1 (as we only consider wind bin 1 for validation of the model). In measurement-based assessments, the DEL is derived based on the un-weighted average of DEL_{10min} assuming that the database is large enough to have the probabilities fairly accounted for automatically. In other words, the probability of the wind conditions is already embedded in forming the distribution of 10-minute DEL measurements. Equation 9 shows the relation between DEL_{10min} and $DEL_{lifetime}$ in case of n number of DEL_{10min} available.

$$\mathrm{E}[DEL^m_{lifetime}] = \sum_{i=1}^{n} \frac{DEL^m_{10min_i}}{n} \tag{9}$$

In Eq. 9, in the case of DEL in one year, n would be the number of 10 minutes within the timeline of 1 year. If enough DEL_{10min} data are not available, one has two options: statistical extrapolation (as in the current study) or assuming that the same observations repeat during the longer times.

2.4.3 Forming the DEL database based on measurements and statistical extrapolation

For the site-specific (measurement-based) assessment of reliability, we need to obtain the distribution of the $\log(DEL_{lifetime})$ in each year to put in Eq. 14 to be able to estimate the annual reliability level up to year 30 using Eq. 16. We prepare the data for such assessments for up to 30 years. To do so, we follow the below procedure:

1. Fitting a distribution to the 10-minute DEL measurements
2. Forming a database based on the distribution and extrapolating to 30-year return loads
3. Taking random 500 samples of size $365 * 24 * 6 * N$ from the database with replacement; N accounting for the year number and repeating from year 1 to 30.
4. Calculating the mean of $(DEL_{10min})^m$ in each of the 500 samples and estimating the corresponding $DEL_{lifetime}$ based on Eq. 9.
5. Calculating the logarithm of all generated data and fitting probability distribution to the 500 realizations of $\log(DEL_{lifetime})$ in each year.

https://doi.org/10.5194/wes-2024-68
Preprint. Discussion started: 28 June 2024

eawe european academy of wind energy
Open Access WIND ENERGY SCIENCE DISCUSSIONS

For forming the database (step 1 above), first, we find the probability of exceedance corresponding to 30-year return period using Eq. 10 and Eq. 11. The return load is the load that can happen once in a duration equal to the return period.

$$CDF(L_R) = \exp\left(\frac{-1}{T}\right) \tag{10}$$

$$Pr_{exc.}(L_R) = \log(1 - CDF(L_R)) \tag{11}$$

In Eq. 10 and Eq. 11, L_R accounts for the return load level, and T in Eq. 10 accounts for the ultimate time of interest. For example, in the current study, we are interested in finding the load that occurs once during 30 years, making the parameter T equal to the number of 10 minutes in 30 years. We set the time in terms of the number of 10 minutes because we consider the DEL to be the load, and in this case, each DEL is an occurrence of a 10-minute duration. The $Pr_{exc.}$ in 11 is the probability of exceedance of such load, meaning the probability that a load higher than that level occurs. In the case of return loads, this probability is normally very low. We use the CDF corresponding to the return period, obtained from Eq. 10, to find the return load in our case. This load can be derived by finding the inverse CDF of the distribution of our 10-minute data (step 1 above). After finding the return load, we can find the number of occurrences of each DEL level in our database based on Eq. 12.

$$i = \frac{1}{\Pr(L_R)} \tag{12}$$

In Eq. 12, i is the number of occurrences of each 10-minute DEL level DEL_{10min_i} and $Pr(L_R)$ is the probability of occurrence of the return load based on the distribution of DEL_{10min}s (distribution in step 1 above). Equation 12 is based on the assumption that the probability density functions of DEL_{10min} remain the same when more observations are added to the tail through time. The more data involved in fitting the distribution of DEL_{10min}, the more accurate this assumption is.

2.4.4 Fatigue reliability estimation

Fatigue reliability assessment is performed to obtain an estimation of the probability of the survival of a structure. Equation 13 presents a mathematical representation of this concept.

$$R(t) = 1 - P_f(t) \tag{13}$$

In Eq. 13, $P_f(t)$ is the probability of failure at time t and can be stated as the probability of exceeding a certain level. Commonly, this problem is referred to with a function named limit state function $(g(x,t))$, and the safe region is where this function is positive. We fully follow the methods and procedures used in our previous work in (Mozafari et al. , 2023c) for reliability estimation. Here, we present a brief introduction and the general approach. We recommend the reader to check (Mozafari et al. , 2023c) for further details.

https://doi.org/10.5194/wes-2024-68
Preprint. Discussion started: 28 June 2024

eawe european academy of wind energy
Open Access WIND ENERGY SCIENCE DISCUSSIONS

Following Miner's rule, failure can happen when damage is higher than a threshold level (commonly 1). This rule contains uncertainty due to simplified assumptions like linear damage accumulation without sequence effect. To account for the uncertainty in Miner's rule, we set the threshold (Δ) as a random variable with a mean value equal to 1. Thus, the reliability being the probability of survival, would be the probability of damage being less than Δ. Equation 14 describes the limit state function considering DEL, K, and Δ as random inputs.

$$g(X) = \log(\Delta) - \log(N_{eq}) - m\log\left(\frac{c}{I}\right) + \log(k) - m\log(DEL_{lifetime}) \tag{14}$$

The parameters $log(N_{eq})$ and $mlog(\frac{c}{I})$ in Eq. 14 are constants. Thus, the above equation consists of three random parameters related to the linear damage accumulation model ($\log(\Delta)$), material Resistance ($\log(k)$), and load ($\log(DEL_{lifetime})$). We perform the probabilistic reliability assessment using FORM analysis in the current work to find the probability that the function g in Eq. 14 can be positive (fatigue reliability). We use the reliability index (shown in Eq. 15) as a commonly used measure of structural reliability.

$$\beta = -\Phi^{-1}(P_f) \tag{15}$$

The operator Φ^{-1} shown in Eq. 15 corresponds to the inverse cumulative distribution function (CDF) of the standard normal distribution.

We consider $R = 10$ for fatigue properties of the composite Mikkelsen (2020).

To apply FORM analysis, first, we fit distributions to the estimations of $\log(DEL_{lifetime})$ calculated based on 10-minute simulations using Eq. (9) for the measurement-based assessment and Eq. (8) for the simulation-based scenarios. For modeling the uncertainty in the model and material properties in the current study, we gather information regards the distributions and statistical parameters from the literature. Table 3 shows this information plus the references for the coefficients of variation.

Table 3. Characteristics of the material and model variables

Variable	Distribution	mean	std	Reference
$log(\Delta)$	Normal	-0.1116	0.4724	Toft and Sørensen (2011); Toft et al. (2016)
$log(K)$	Normal	calibrated	0.528	Fraisse and Brøndsted (2017)

Equation 16 and Eq. 17 present the formulations for calculating the annual probability of failure and an annual reliability index based on survival in the year before (for further information, see Faber, M. H. (2012)).

$$\Delta P_f(X,t) = \frac{P_f(X,t+\Delta t) - P_f(X,t)}{(1 - P_f(X,t))} \tag{16}$$

https://doi.org/10.5194/wes-2024-68
Preprint. Discussion started: 28 June 2024

eawe european academy of wind energy
Open Access WIND ENERGY SCIENCE DISCUSSIONS

$$\Delta\beta(X,t) = -\Phi^{-1}(\Delta P_f(X,t)) \tag{17}$$

3 Results and discussions

We validate the model of the turbine before performing the study (see Appendix for validation results). The current section presents the results in three parts: Turbulence comparison (Sect. 3.1), fatigue load comparison (Sect. 3.2), and fatigue reliability comparison (Sect. 3.3). The reliability assessment also includes the sensitivity of the reliability level to different random inputs at the target extended life (30 years) in all approaches. Finally, we present the overall discussions on the results in Sect. 3.4.

3.1 Comparison of turbulence levels

Figure 2 presents the comparison between site-specific turbulence based on SCADA data, the Frandsen model, and the IEC design class in different wind direction bins. The plot of each direction bin only includes the mean wind speed bins in which there are enough available data to cover the comparison. The box plots in Fig. 2 contain the data from 25% quantile up to 75% quantile, and the red 'plus signs'account for data in the high and low tails and possible outliers.

The scatter of the turbulence versus the corresponding 10-minute DEL measurements in different direction bins are provided in the appendix (see Fig. D1 for precise observation of the placing of the high turbulence points related to the cluster of data). If we consider no outlier in turbulence measurements and approve the data as they are, according to Fig. 2 in the wind bin 1 (free stream condition), the Frandsen model and IEC design level turbulence underestimate the site turbulence in low mean wind speeds while overestimating it in high mean wind speeds (over the rated speed). Emeis (2014) claims the same results for the case of design-level turbulence. This trend remains the same almost in all other wind direction bins. Direction bins 2 and 4 include very high wake effects and high turbulence levels and show less conservative assumptions by the IEC class and the Frandsen model in even high mean wind speeds. Figure 2 reveals that in some cases, the Frandsen model does not produce much higher turbulence compared to the IEC design representative turbulence for the class. In the following section, we investigate the differences in terms of fatigue loads and fatigue reliability as more accurate parameters to estimate the lifetime extension based on each turbulence estimation approach.

3.2 $DEL_{lifetime}$ distributions

As shown in Eq. 14, finding the distribution of $log(DEL_{lifetime})$ is a necessity for estimating the probability of failure. The current section presents the distribution of $DEL_{lifetime}$ and $log(DEL_{lifetime})$ based on measurement data (DEL_{10-min}). First, we observe the empirical probability distribution of the 10-minute DEL measurements, from which we evaluate $DEL_{lifetime}$ realizations. Fig. 3 shows the empirical probability density of the 10-minute damage equivalent flapwise moment from measurement data.

https://doi.org/10.5194/wes-2024-68
Preprint. Discussion started: 28 June 2024

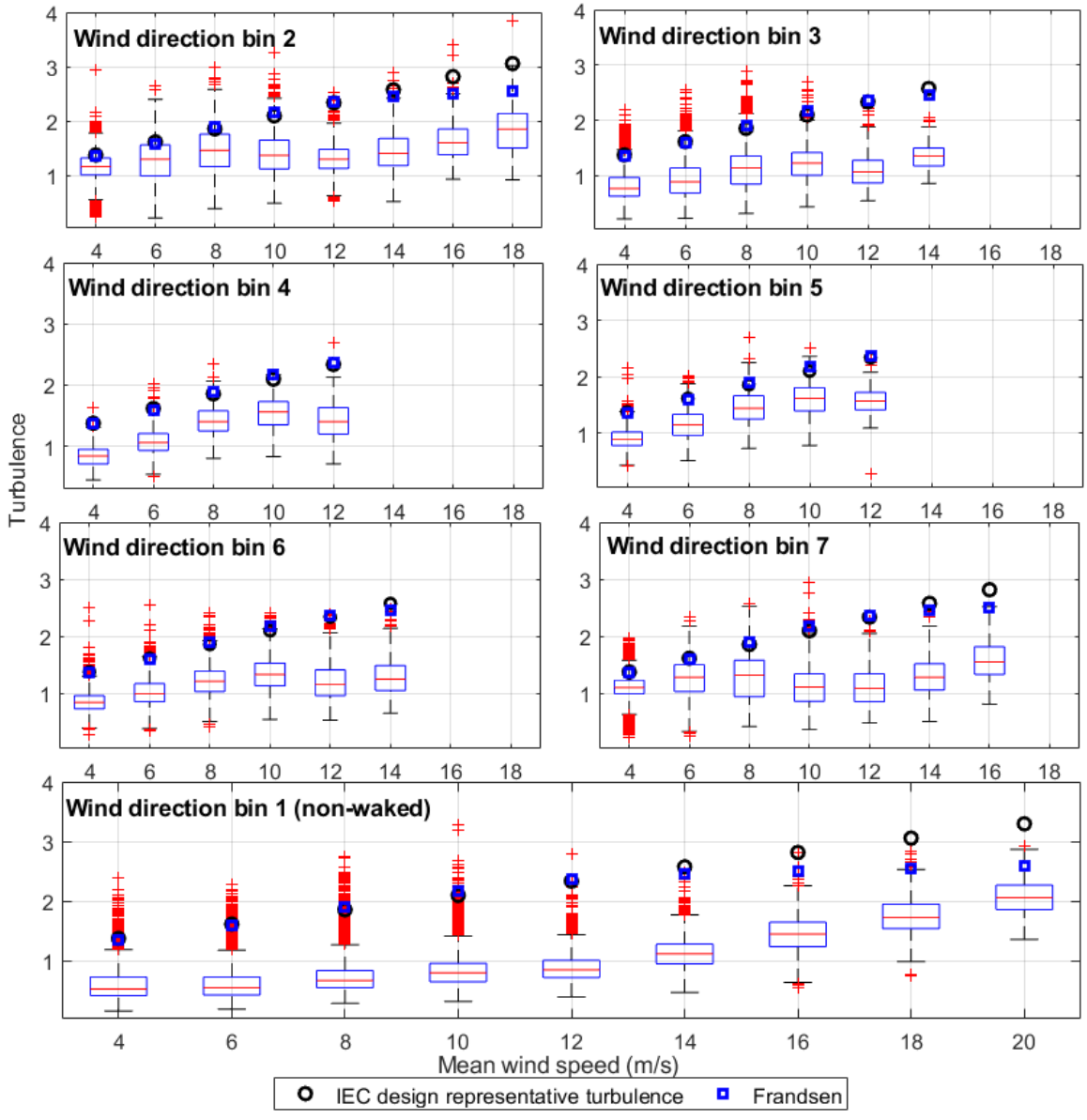

Figure 2. The enhanced turbulence based on Frandsen estimation (blue squares) compared with IEC design representative turbulence (black circles) and the site turbulence measurements (box plots)

As Fig. 3 reveals, the distribution of the 10-minute DEL data is multi-modal and cannot be represented fully by uni-modal distributions. The multi-modality of the DEL can be a result of having both stratified and un-stratified winds during the observation time, as the same behavior can be seen in each wind direction bin (see Fig. D2 in the appendix). We investigate the mixture of two or three Gamma distributions as well as a mixture of two or three Gaussian distributions as the candidates.

https://doi.org/10.5194/wes-2024-68
Preprint. Discussion started: 28 June 2024

eawe european academy of wind energy
Open Access WIND ENERGY SCIENCE DISCUSSIONS

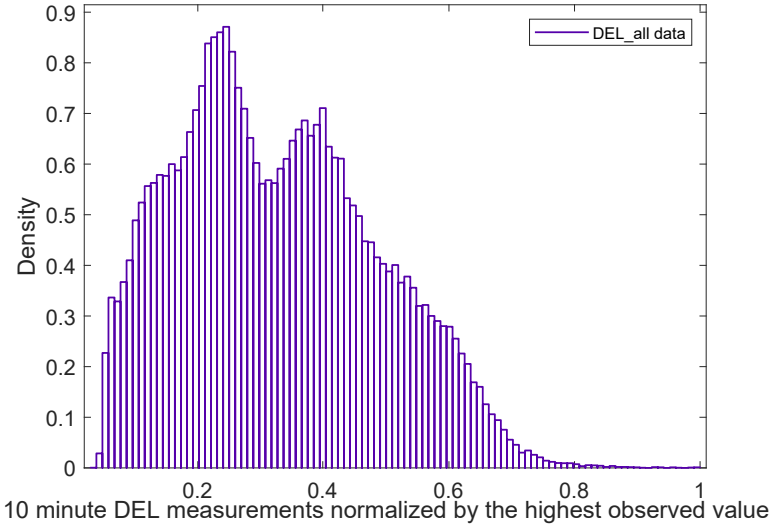

Figure 3. Empirical probability density of the 10-minute DEL measurements in all mean wind speed directions combined

Among all, the mixture of two Gamma distributions appears to be the best fit to describe the statistical behavior of the 10-minute damage equivalent flapwise moments in the case study wind turbine's blade root (in all direction bins combined). Fig. 4 shows this fit on the empirical CDF of data.

As Fig. 4 presents, the Gamma mixture model fits the data well with fair accuracy in the higher tail. We use the probability of exceedance from this model and follow the steps presented in 2.4.3, to find the return load corresponding to 30 years. We use Eq. 10 and Eq. 11 to extrapolate the distribution to a 30-year return load. The slow growth of the tail from year 5 (corresponding to the probability of the largest data observed) to 30 years shows that the distribution is fairly converged, and a five-year return period is enough for the main assumption in Sect. 2.4.3 to hold. Continuing the procedure with bootstrapping as outlined in section 2.4.3, the realization of $DEL_{lifetime}$ in different years is shown in Fig. 5.

As shown in Fig. 5, the mean value of the realizations converges as the standard deviation decreases. This complies with our expectation according to the law of large numbers: The mean converges to the 'true' expected value of $DEL_{lifetime}$ as we gather more observations through the years. The change in the standard deviation with a slight change in the mean value allows for the assumption of non-linear damage accumulation through time (variable DEL through time). We use the converged distribution of $DEL_{lifetime}$ for the estimation of the annual reliability index.

Fig. 6 presents the PDF of $DEL_{lifetime}$ in two different turbulence scenarios of the IEC 61400-1 representative design value and the Frandsen estimation using bootstrapped data among simulations. The data in 6 are normalized by the converged mean of $DEL_{lifetime}$ obtained above using site measurements.

As Fig. 6 reveals, the estimation of the $DEL_{lifetime}$ based on the representative turbulence for design and the Frandsen estimation are conservative compared to the site-specific assessment based on measurements. The Frandsen model, in this case,

https://doi.org/10.5194/wes-2024-68
Preprint. Discussion started: 28 June 2024

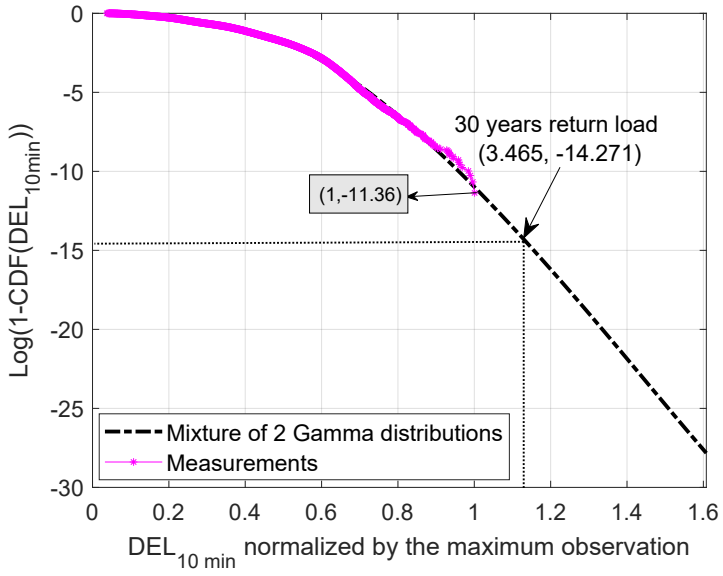

Figure 4. Probability of the exceedance of the DEL based on empirical cumulative distribution function (purple stars) and based on best distribution fit to the data (black dashed line)

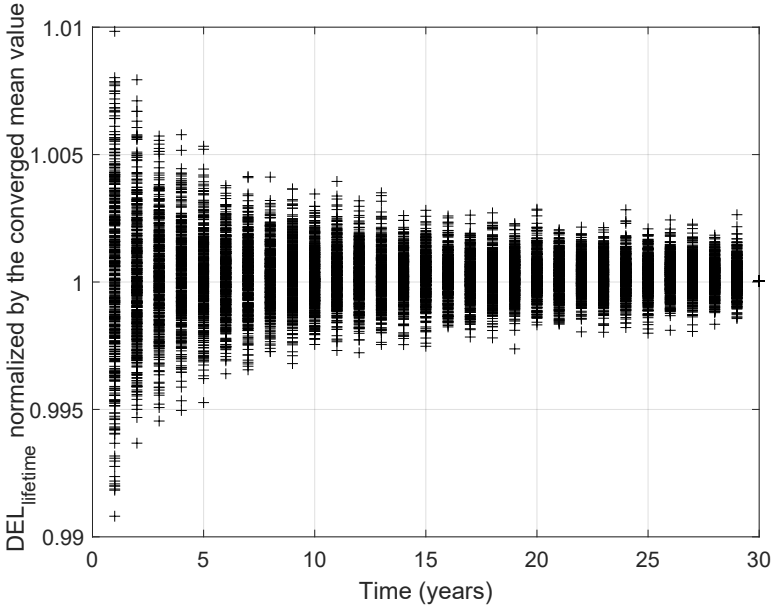

Figure 5. The realizations of $DEL_{lifetime}$ generated via bootstrapping of available 10-minute DEL estimates through years

https://doi.org/10.5194/wes-2024-68
Preprint. Discussion started: 28 June 2024

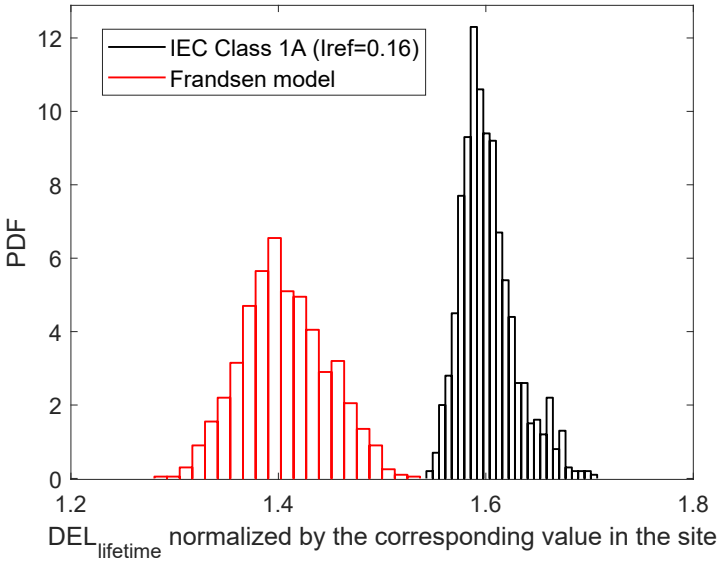

Figure 6. PDF of $DEL_{lifetime}$ in two different scenarios of the IEC standard for design and site-suitability check (based on the Frandsen model) normalized by the mean $DEL_{lifetime}$ estimation based on site's measurements

leads to respectively less conservative fatigue loads than design-based approach as expected. In addition, the DEL realizations based on the Frandsen model are more spread, showing a higher variability. In the following section, we use the $DEL_{lifetime}$ distribution for assessing the fatigue reliability at the end of the design service life and the possible extended life in different scenarios.

3.3 Reliability and importance ranks

As the model is generic and the material properties are not defined accurately, we assess the lifetime extension after calibrating the material's mean strength. The calibration is made such that we get the target annual reliability index level for a moderate consequence of the failure of a structural component (equal to 3.7) (IEC 61400-1 , 2019) at the end of design life (20 years). Fig. 7 presents the annual reliability index for 35 years in all three case scenarios based on the calibrated material properties.

The difference in the annual reliability levels in different scenarios in Fig. 7 is due to the difference in the turbulence, observed in Sect. 3.1. The reliability of 3.7 at year 35 for the Frandsen model means there is a possibility of a lifetime extension of up to 10 years for the turbine under study when using this model. Using the site data, this level is reached in more years, showing the conservative results from the Frandsen model. The fast drop in the design-based annual reliability in Fig. 7 represents the high mean value of the design DEL compared to the Frandsen model and site. The high difference between the reliability in the three scenarios is due to the high fatigue exponent of the composite increasing the effect of the mean of

https://doi.org/10.5194/wes-2024-68
Preprint. Discussion started: 28 June 2024

eawe european academy of wind energy
Open Access WIND ENERGY SCIENCE DISCUSSIONS

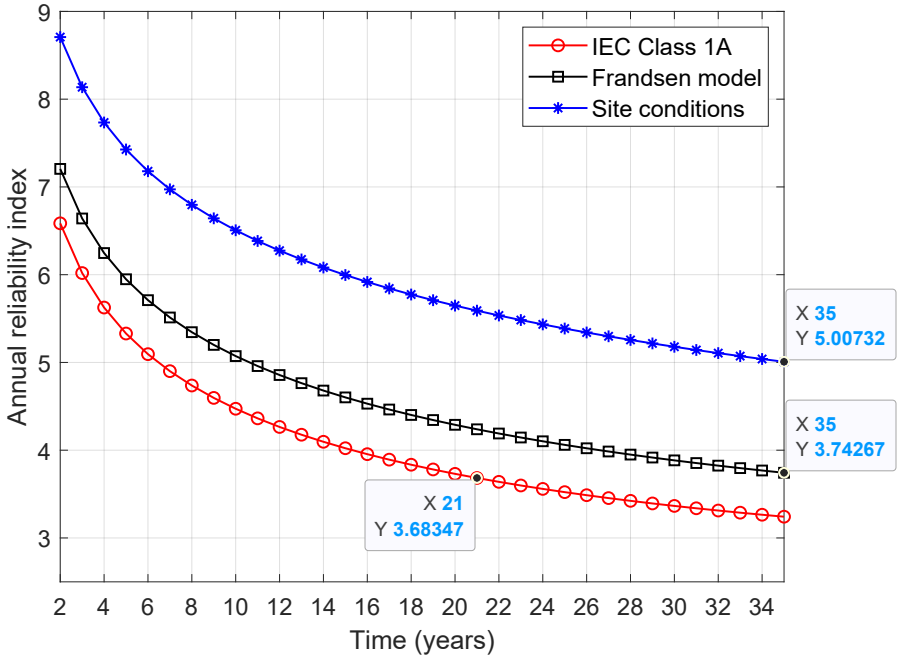

Figure 7. Annual reliability of the case study wind turbine in three scenarios of using Frandsen model (black square), IEC design class (red circle), and site measurements with (blue)

365 fatigue loads on the reliability.

Table 4 shows the importance rank of the random variables in the limit state function (see Eq. 14) based on FORM analysis.

Table 4. The sensitivity of the reliability to different random variables (%) based on three approaches at year 30

Random variables / Assessment basis	Frandsen model	IEC design-level	Site measurements
$log(\Delta)$	38.29	41.70	44.46
$log(K)$	47.84	52.09	55.54
$log(DEL_{lifetime})$	13.87	6.21	7.62e-3

As Table 4 reveals, the relative importance of the load is low in all three scenarios. The relative importance of the fatigue load is higher in the case of the Frandsen model because of the high coefficient of variation of the DEL in this case. Its sensitivity to loads is almost zero when it comes to the site-specific lifetime DEL. The effects of the uncertainty in the material properties are
370 the highest in all cases because of the very high coefficient of variation. In the site assessment, the reliability is highly sensitive firstly to the material uncertainty and secondly to the damage accumulation rule.

https://doi.org/10.5194/wes-2024-68
Preprint. Discussion started: 28 June 2024

eawe european academy of wind energy
Open Access WIND ENERGY SCIENCE DISCUSSIONS

3.4 Discussion

The data show the conservative estimations of turbulence based on the Frandsen model in high mean wind speeds and, thus, in the overall DEL estimations when considering the blade's flapwise bending moments. The reliability assessments show the possibility of a lifetime extension for more than 35 years while maintaining safety margins.

The very low sensitivity of the reliability to the fatigue loads in the case of site-specific assessment is due to the relatively low coefficient of variation of this variable compared to material strength and Miner's rule. This shows the robustness of $DEL_{lifetime}$ as an accumulated/averaged random variable. The results comply well with the results shown in (Mozafari et al. , 2023b) showing how the accumulation decreases the coefficient of variation of $DEL_{lifetime}$.

There are some limitations and simplifications in the present study that must be considered and improved in future work. As an example, there is a potential difference in the results of the simulation-based approaches if the model was not generic. The results of the model validation show that the small differences in load can lead to underestimation of the $DEL_{lifetime}$ in simulation-based scenarios and, thus, the remaining service life. This is especially important in the assessment based on Frandesn model as the sensitivity studies show that the reliability of the Frandsen-based approach is sensitive to the loads.

In addition, the results of the current study are performed on the blade flapwise load channel as a case-study. However, all the load channels shall be investigated for lifetime extension estimation. Furthermore, load channels with deterministic behaviour (for example blade edgewise moments) often have lower design margins and thus are the critical components deriving the lifetime extension of the wind turbine. The current study is not focusing on actual lifetime of the turbine and focuses on showing the difference between Frandsen site-suitability assessment and assessments based on measurements when it comes to Fatigue reliability. Such comparison is more clear on a turbulence-driven fatigue load like flapwsie bending moment.

Furthermore, although the turbulence levels from site and the Frandsen estimation are directly compared, the fatigue load results based on the two are derived differently. The former is based on post-processing of strain-gauge data and the later based on aeroelastic simulations. Thus, the possible bias and errors of the turbine model and aeroelastic simulations can affect the DEL and reliability comparison results.

For future studies, we recommend below studies:

1. Performing the same study on the performance of the Frandsen model in deeper locations within the wind farm, as they usually include more intense/complicated wake conditions
2. Investigating the effects of using ambient wind data (using Frandsen) instead of local on-site measurements of the waked turbulence considering all the load channels (lifetime extension assessment as a whole).

https://doi.org/10.5194/wes-2024-68
Preprint. Discussion started: 28 June 2024

3. considering other sources of uncertainty in the reliability assessment framework, including the uncertainty due to the range counting methods, uncertainty in simulations, etc.

4. Investigating the reasons behind the multi-modality of the 10-minute DEL distribution.

5. Performing the same study using independent fittings and extrapolations of DEL in each wind bin for higher certainty and accuracy in the assessment.

6. Joining the study with inspection and health-monitoring data coupled with risks and cost analysis to obtain a complete set of tools for decision-making regarding lifetime extension.

4 Conclusions

The present research investigates the effects of using the Frandsen model for estimation of effective turbulence in a compact wind farm layout with mixed-wake conditions. The investigation is done on three levels: investigation of turbulence estimates, fatigue loads estimates, and reliability estimates through time. In addition, the sensitivity of the reliability index to the uncertainty from three inputs of loads, material properties, and Miner's rule is studied in different approaches of design-based and site-specific assessment. The results reveal the difference between the lifetime extension assessment based on Frandsen's simplified model and site-specific conditions considering blade flapwise moments. The study is based on a single turbine within the Lillgrund wind farm with a few years of measurement data from a strain gauge. The reliability assessment accounts for the variations in the turbulence as well as DEL using site measurements and statistical extrapolation of the fatigue loads. h and more than ten years based on the probabilistic model built using measurements. The results of the study show a 35% higher reliability index at the end of 35 years when using site measurements compared to estimations based on the Frandsen model. Considering prolonged variations of the reliability index at the high lifetimes, this equals many years of difference in the expected lifetime after 35 years. The sensitivity of the reliability and, thus, the lifetime extension assessment is highly sensitive to the material properties. In addition, the relative importance of the loads in assessments based on the Frandsen model is higher than in design or assessments based on-site measurements.

The procedure for anticipation of the probability of the DEL through lifetime will help the stakeholders and wind farm owners to get a better assessment of the fatigue damage in cases where strain gauge measurements are not available or are only available for a short span of the turbine's lifetime. Reassuring the performance of the Frandsen model for safe assessment of the site suitability in the case of compact wind farms with irregular arrangements is valuable information, as the general applications of the Frandsen model are still unclear.

https://doi.org/10.5194/wes-2024-68
Preprint. Discussion started: 28 June 2024

eawe european academy of wind energy
Open Access WIND ENERGY SCIENCE DISCUSSIONS

Appendix

1 Model Validation

As mentioned in Sect. 2.3.2, group 3 simulations are for validation of the model. The input of this group is based on site-specific inputs from the non-waked free stream (wind direction bin 1). First, we compare the mean load levels from the measurements in wind bin 1 to the results of the group 3 simulation. Then, we compare the 10-minute DEL evaluations and investigate the differences in $DEL_{lifetime}$ formed via bootstrapping.

Figures A1 and B1 show the comparison of the mean load levels and 10-minute DELs in the measurements versus simulations, respectively.

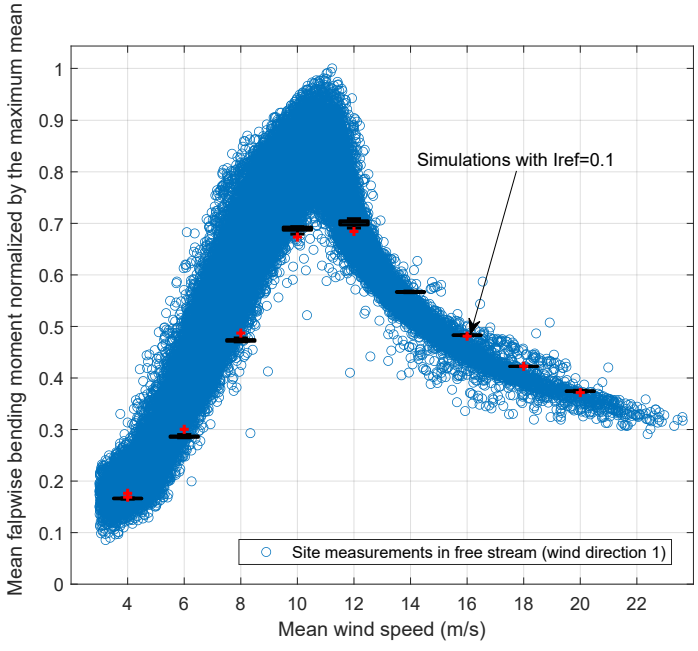

Figure A1. The mean flapwise bending moment in different mean wind speeds in non-waked directions from two sources of measurements (blue circles) and simulations (black boxplots)

Table A1. Statistical parameters of $DEL_{lifetime}$ according to the non-waked aeroelastic simulations using site-specific turbulence and shear exponent versus the same parameters from measurements

Source	Mean DEL normalized by the mean based on measurements	std of the $DEL_{lifetime}$
Site-specific simulations for non-waked area	1	0.014
Measurements for non-waked area	1.04	0.031

https://doi.org/10.5194/wes-2024-68
Preprint. Discussion started: 28 June 2024

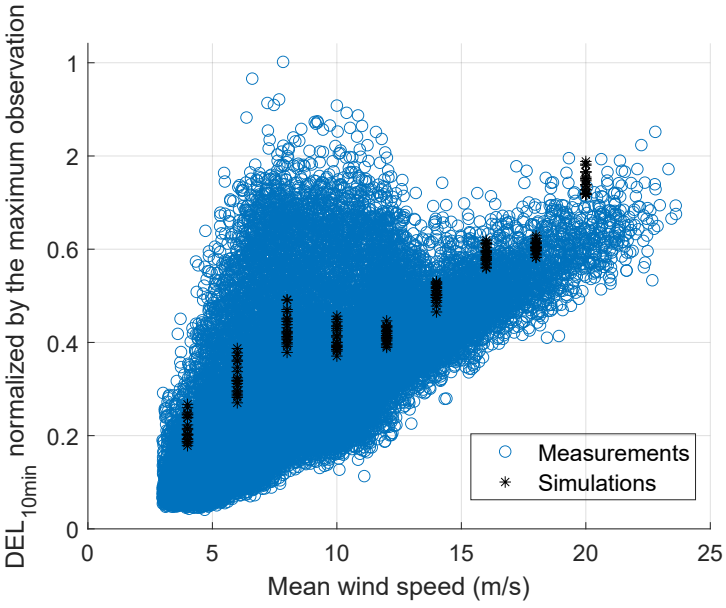

Figure B1. The cluster of 10-minute DEL data in the free stream versus the DEL estimations from simulations in each mean wind speed

The data shown in Figure A1 and B1 reveal the high variation in the measured mean load and damage equivalent flapwise moment around rated mean wind speed. The high difference in this area can introduce some errors in the estimations based on simulations (groups 1 and 2) based on dominant (high probability) wind speeds. However, generally, the data shows fair coverage of the site load behaviors.

In addition, the data in table A1 reveals that the load fluctuations in the simulations are very small compared to reality. This is partly because of the integration over turbulence distribution (see (Mozafari et al. , 2023c) for details) and partly due to the variability of the environmental condition (see Sect. 3.1). In the following sections, we compare the turbulence levels in three scenarios of the study. Although the validations show over-estimations of the load and DEL in high mean wind speeds, we proceed with the study using the available HAWC2 model because the difference in the overall DELs shown in Table A1 are less.

Fig. B1 shows the scatter of the available DEL data for the current study during the 5 years of the corresponding measurement campaign.

Fig. C1 represents the power production versus mean wind speed compared with the nominal power curve after filtration.

Different distributions shown in the table below are fitted to the mean wind speed data of the wind turbine. As can be seen, the best fit is the Rayleigh distribution. The maximum likelihood method is used for fitting and the prediction error is measured by Akaike information criterion (AIC).

Fig. D1 shows that the high tail of turbulence observations mostly belongs to the cluster of data, and the possibility of having a high number of outliers is low. The probability of exceedance of the 10-minute DEL measurements within each wind

https://doi.org/10.5194/wes-2024-68
Preprint. Discussion started: 28 June 2024

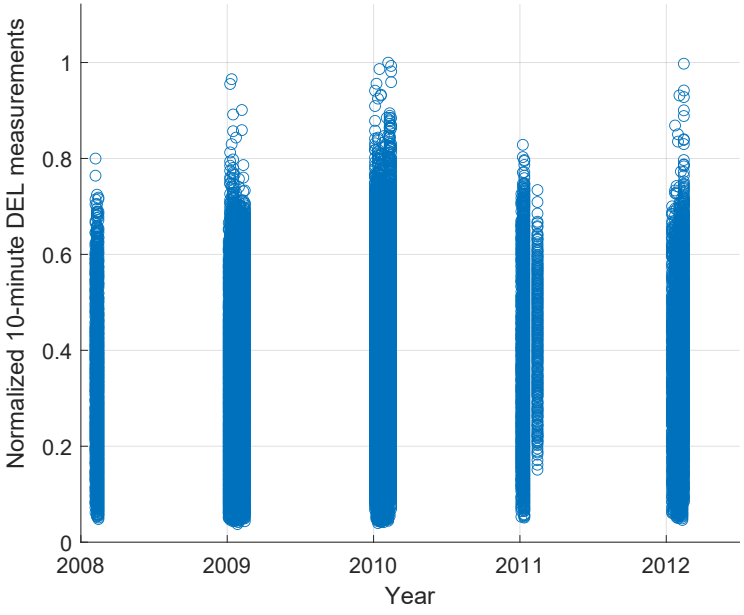

Figure B1. The scatter of 10-minute measurements during 5 years in terms of corresponding DEL evaluations normalized by the highest estimation

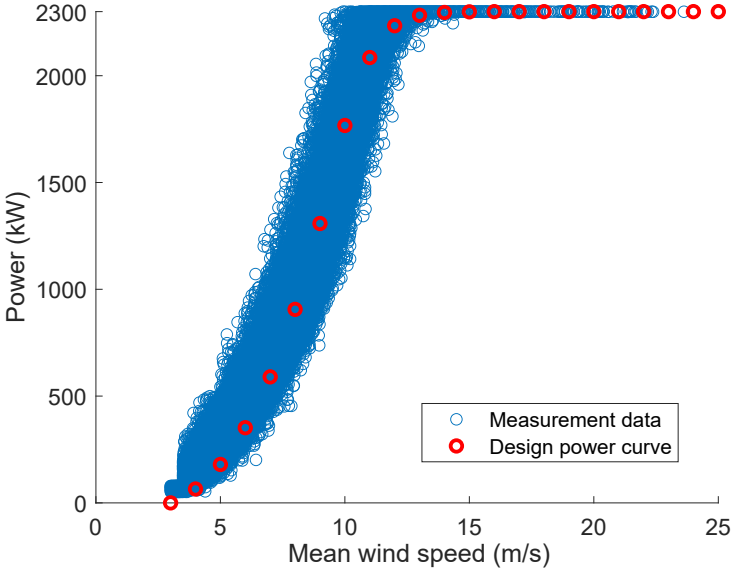

Figure C1. The filtered power production data versus mean wind speed (blue) compared with the nominal power curve (red)

https://doi.org/10.5194/wes-2024-68
Preprint. Discussion started: 28 June 2024

eawe european academy of wind energy
Open Access WIND ENERGY SCIENCE DISCUSSIONS

Table D1. different distribution fits to the wind speed data measurements

Distribution	Par1	Par2	Par3	Log-Likelihood	AIC
Rayleigh	5.90			-7.23E+05	1.45E+06
Gev	-0.12	3.70	5.47	-7.25E+05	1.45E+06
Normal	7.23	4.17		-7.32E+05	1.46E+06
Gamma	3.00	2.41		-7.40E+05	1.48E+06
exponential	7.23			-7.65E+05	1.53E+06
Ev	9.39E+00	4.560		-7.68E+05	1.54E+06
Uniform	0.00	2.81E+01		-8.57E+05	1.71E+06

direction bin is shown in Fig. D2 using both the empirical CDF and the best distribution fit to each cluster of data.

460 Figure D2 shows that the highest DEL observations occur in wind bin 5.

https://doi.org/10.5194/wes-2024-68
Preprint. Discussion started: 28 June 2024

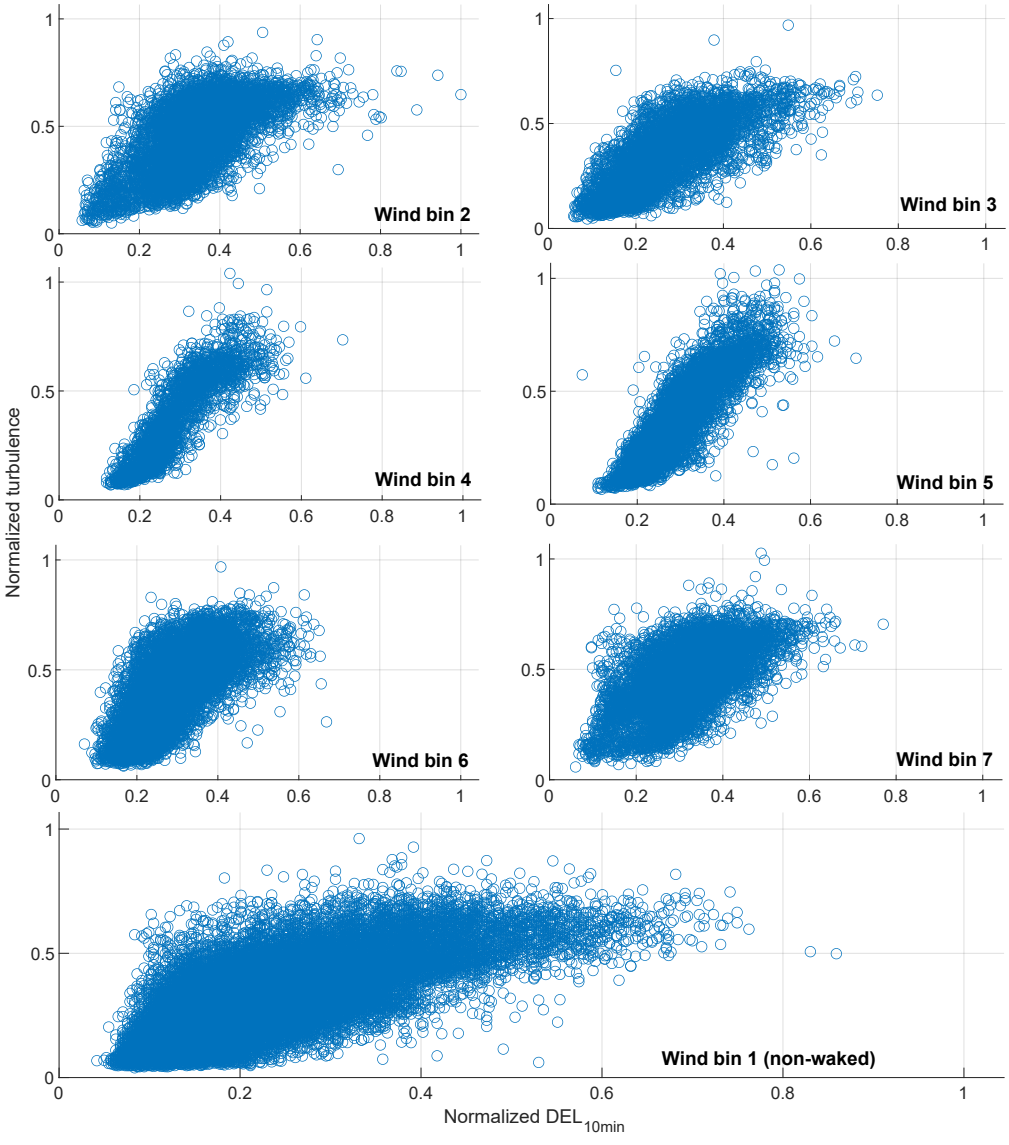

Figure D1. Scatter plot of turbulence data normalized by the highest observations versus corresponding 10-minute DEL observations at the same time in different wind direction bins before filteration

https://doi.org/10.5194/wes-2024-68
Preprint. Discussion started: 28 June 2024

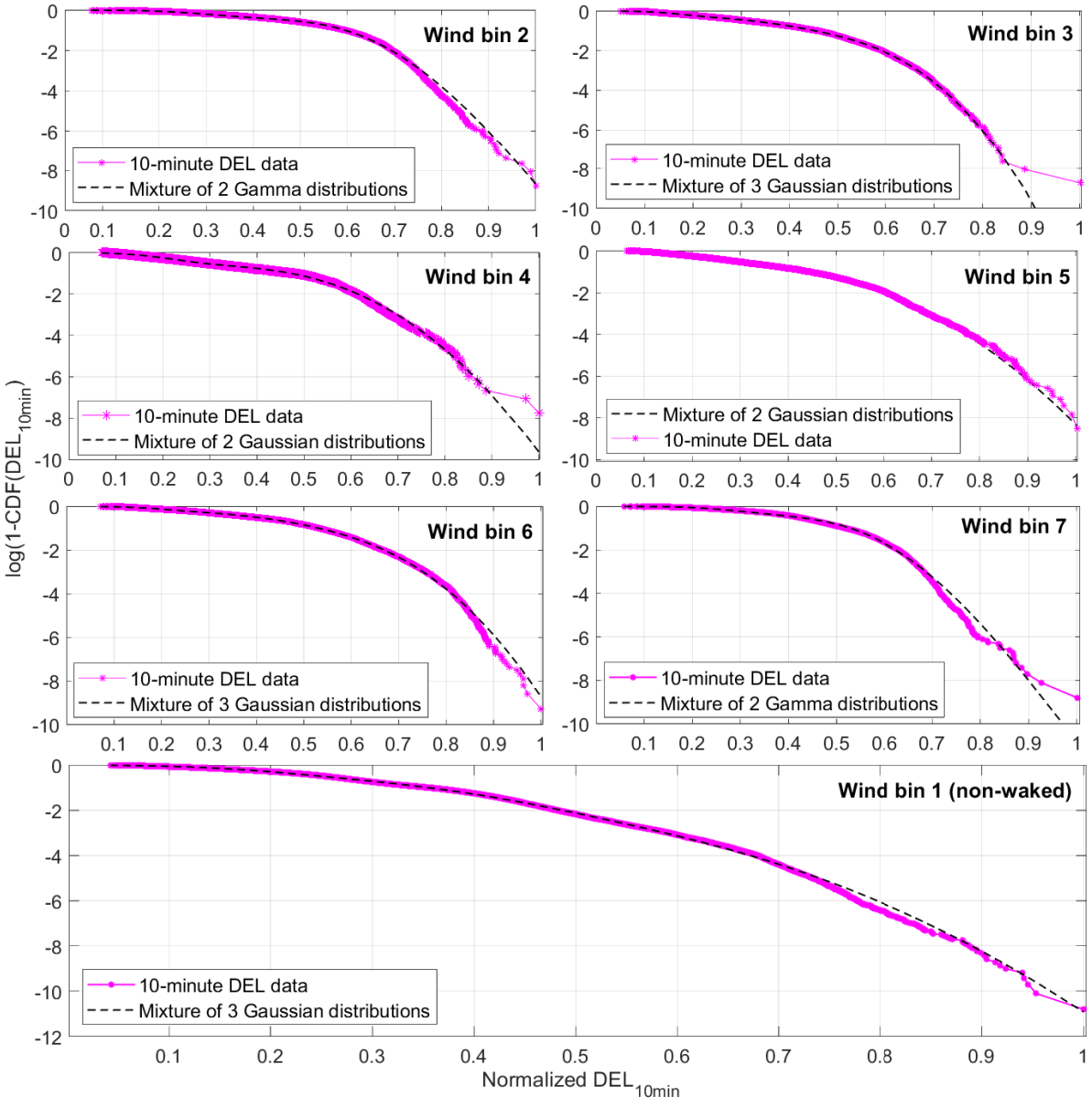

Figure D2. Probability of exceedance of the normalized in different wind direction bins in the location of the wind turbine and the best distribution fits

https://doi.org/10.5194/wes-2024-68
Preprint. Discussion started: 28 June 2024

eawe european academy of wind energy
Open Access WIND ENERGY SCIENCE DISCUSSIONS

Author contributions. SM, JR, and PV were responsible for the overall conceptualization of the study. SM wrote all the computer codes and performed all the data analysis. SM, PV, and KD were involved in the writing and editing of the manuscript

Competing interests. At least one of the (co-)authors is a member of the editorial board of Wind Energy Science.

https://doi.org/10.5194/wes-2024-68
Preprint. Discussion started: 28 June 2024

References

Amiri, A. K., Kazacoks, R., McMillan, D., Feuchtwang, J., and Leithead, W.: Farm-wide assessment of wind turbine lifetime extension using detailed tower model and actual operational history, Journal of Physics: Conference Series, vol. 1222, p. 012034, IOP Publishing, 2019.

Argyle, P., Watson, S., Montavon, C., Jones, I., and Smith, M.: Modelling turbulence intensity within a large offshore wind farm, Wind425 Energy, 21, 1329–1343, 2018.

Basquin, O.: The Exponential Law of Endurance Tests, ASTM, p. 625, 1910.

Bayo, R. T. and Parro, G.: Site suitability assessment with dynamic wake meandering model. A certification point of view, Energy Procedia, 76, 177–186, 2015.

Faber, M. H.: Statistics and probability theory: in pursuit of engineering decision support, Springer Science and Business Media, Vol. 18, London, 2012.

Commission, G. I. E.: IEC 61400-1, Wind turbine generator systems – Part 1: Safety requirements, 3rd edition ed, Proceedings of the IEC, pp. 61 400–3, 2005.

Commission, G. I. E.: IEC 61400-1, Wind turbine generator systems – Part 1: Safety requirements, 4th edition ed, Proceedings of the IEC, pp. 61 400–4, 2019.

Dahlberg, J.: Assessment of the Lillgrund Windfarm. 6-1 LG Pilot Report, 2009.

Dimitrov, N. and Natarajan, A.: From SCADA to lifetime assessment and performance optimization: how to use models and machine learning to extract useful insights from limited data, Journal of Physics: Conference Series, vol. 1222, p. 012032, IOP Publishing, 2019.

Dimitrov, N., Natarajan, A.: Probabilistic framework to quantify the reliability levels of wind turbine structures under enhanced control methods Deliverable D2.5, 2020.

ISO, I. "2394." General Principles on Reliability for Structures.—1994.—50p, 2015.

Emeis, S.: Current issues in wind energy meteorology, Meteorological Applications, 21, 803–819, 2014.

Endo, T., Mitsunaga, K., and Nakagawa, H.: Fatigue of metals subjected to varying stress-prediction of fatigue lives, Preliminary Proceedings of the Chugoku-Shikoku District Meeting, pp. 41–44, The Japan Society of Mechanical Engineers, 1967.

Fraisse, A. and Brøndsted, P.: Compression fatigue of Wind Turbine Blade composites materials and damage mechanisms, Proceedings of the 21st International Conference on Composite Materials (ICCM-21), Xi'an, China, pp. 20–25, 2017.

Frandsen, S.: Turbulence and turbulence generated loading in wind turbine clusters, Risø report R-1188, 2007.

Frandsen, S. T. and Madsen, P. H.: Spatially average of turbulence intensity inside large wind turbine arrays, European seminar offshore wind energy in Mediterranean and other European seas, pp. 97–106, Univ. of Naples, 2003.

Natarajan A, Dimitrov NK, Peter DR, Bergami L, Madsen J, Olesen NA, Krogh T, Nielsen JS, Sørensen JD, Pedersen M, Ohlsen G.: Demonstration of requirements for life extension of wind turbines beyond their design life, 2020.

Hübler, C., Weijtjens, W., Rolfes, R., and Devriendt, C.: Reliability analysis of fatigue damage extrapolations of wind turbines using offshore strain measurements, Journal of Physics: Conference Series, vol. 1037, p. 032035, IOP Publishing, 2018.

Kim, S.-H., Shin, H.-K., Joo, Y.-C., and Kim, K.-H.: A study of the wake effects on the wind characteristics and fatigue loads for the turbines in a wind farm, Renewable Energy, 74, 536–543, 2015.

Larsen, T. J. and Hansen, A. M.: How 2 HAWC2, the user's manual, target, 2, 2007.

Le, X. and Peterson, M.: A method for fatigue-based reliability when the loading of a component is unknown, International Journal of Fatigue, 21, 603–610, 1999.

https://doi.org/10.5194/wes-2024-68
Preprint. Discussion started: 28 June 2024

Lee, S., Churchfield, M., Moriarty, P., Jonkman, J., and Michalakes, J.: A numerical study of atmospheric and wake turbulence impacts on wind turbine fatigue loadings, Journal of Solar Energy Engineering, 135, 2013.

Ling, Y., Shantz, C., Mahadevan, S., and Sankararaman, S.: Stochastic prediction of fatigue loading using real-time monitoring data, International Journal of Fatigue, 33, 868–879, 2011.

Mann, J.: Wind field simulation, Probabilistic Engineering Mechanics, 13(4), pp.269-282, 1998.

Megavind: Strategy for Extending the Useful Lifetime of a Wind Turbine, Tech. Rep., 2016.

Mikkelsen, L. P.: The fatigue damage evolution in the load-carrying composite laminates of wind turbine blades, Fatigue Life Prediction of Composites and Composite Structures, pp. 569–603, Elsevier, 2020.

Miner, M. A.: Cumulative damage in fatigue, 1945.

Montavon, C., Jones, I., Staples, C., Strachan, C., and Gutierrez, I.: Practical issues in the use of CFD for modeling wind farms, Proc European Wind Energy Conference, 2009.

Mozafari, S., Dykes, K., Marie Rinker, J., and Veers, P. S.: Extrapolation of the rainflow-counted load ranges for fatigue assessment of the wind turbine's blades, AIAA SciTech 2023 Forum, p. 1541, 2023.

Mozafari, S., Dykes, K., Rinker, J. M., and Veers, P.: Effects of finite sampling on fatigue damage estimation of wind turbine components: A statistical study, Wind Engineering, p. 0309524X231163825, 2023.

Mozafari S, Veers P, Rinker J, Dykes K.: Sensitivity analysis of wind turbine fatigue reliability: effects of design turbulence and the Wöhler exponent, Wind Energy Science Discussions, 1-31, 2023.

Natarajan, A.: Damage equivalent load synthesis and stochastic extrapolation for fatigue life validation, Wind Energy Science, 7, 1171–1181, 2022.

Palmgren, A.: Die lebensdauer von kugellargern, Zeitshrift des Vereines Duetsher Ingenieure, 68, 339, 1924.

Toft, H. S. and Sørensen, J. D.: Reliability-based design of wind turbine blades, Structural Safety, 33, 333–342, 2011.

Toft, H. S., Svenningsen, L., Sørensen, J. D., Moser, W., and Thøgersen, M. L.: Uncertainty in wind climate parameters and their influence on wind turbine fatigue loads, Renewable Energy, 90, 352–361, 2016.

Vitulli, J., Larsen, G. C., Pedersen, M., Ott, S., and Friis-Møller, M.: Optimal open-loop wind farm control, Journal of Physics: Conference Series, vol. 1256, p. 012027, IOP Publishing, 2019.

Ziegler, L. and Muskulus, M.: Fatigue reassessment for lifetime extension of offshore wind monopile substructures, Journal of Physics: Conference series, vol. 753, p. 092010, IOP Publishing, 2016.